ELSEVIER

Journal of Nuclear Materials 290–293 (2001) 639–643

journal of nuclear materials

www.elsevier.nl/locate/jnucmat

Electric currents in the scrape-off layer in ASDEX Upgrade

A. Kallenbach *, A. Carlson, G. Pautasso, A. Peeters, U. Seidel, H.-P. Zehrfeld, ASDEX Upgrade Team

Max-Planck-Institut für Plasmaphysik, IPP–EURATOM Association, Boltzmannstrasse 2, D-85748 Garching, Germany

Abstract

Scrape-off layer (SOL) currents are measured by means of Langmuir probes and shunts in the divertor of ASDEX Upgrade. They consist of the overlayed contributions of thermoelectric and Pfirsch–Schlüter (PS) currents. The SOL currents exhibit a drastic decrease when the line-averaged density approaches the Greenwald density in the H-mode. An analytical model is presented which reproduces the measured thermoelectric current quantitatively. Matching of the analytical model with the measured current scaling yields information about divertor temperatures and SOL e-folding lengths. © 2001 Elsevier Science B.V. All rights reserved.

Keywords: Scrape-off layer; Plasma edge; Sheath

1. Introduction

Electric currents in the scrape-off layer (SOL) of Tokamak plasmas are known for a long time [1]. These currents can be caused via thermoelectric effects by the temperature difference between the two SOL ends [2,3], by Pfirsch–Schlüter (PS) currents [4,5] or by external biasing. A survey on the various experimental observations is given in [6], a comparison with modeling can be found in [7]. Current measurements integrated over the target by shunts provide very robust and reliable data. In this paper, we investigate which quantities of interest can be derived from the measurements.

2. Origin and characteristics of SOL currents

SOL currents are routinely measured in ASDEX Upgrade via shunts connected to divertor target modules in three different toroidal locations. Fig. 1 shows the current measured in one tile of the inner and outer divertor strike point module, respectively. The total current is obtained by multiplying with the number of tiles (64 in case of these modules), while toroidal symmetry is checked by independent measurements in three different toroidal positions. As typical of standard B_t (clockwise from top) and I_p (counter-clockwise) directions, the net target current flows out of the outer and into the inner target.

The current density profile $j_0(\rho)$ in the outer divertor for the discharge of Fig. 1 measured by Langmuir probes kept at target plate potential is shown below in Fig. 3. The profile is obtained by strike point sweeping, the overlap of neighboring probes is quite good. The data were smoothed over 20 ms to average over ELMs in this attached, natural density H-mode discharge. For typical ASDEX Upgrade experimental conditions, the current profile is dominated by the contribution of the thermocurrent, the negative dip inside the separatrix is attributed to PS currents. A corresponding positive PS current feature, overlayed to the thermocurrent inside the separatrix is expected to compensate the negative current in the net target current measured by the shunts: Since the PS currents are driven by the pressure gradient, they change sign around the separatrix and their net contribution will cancel over an individual target as long as the pressure goes to zero along the plate and the target is electrically conducting. Generally, the shunt measurements and the direct j_0 measurement with Langmuir probes at target plate potential give very

* Corresponding author. Tel.: +49-89 3299 1721; fax: +49-89 3299 1812.

E-mail address: arne.kallenbach@ipp.mpg.de (A. Kallenbach).

PII: S0022-3115(00)00445-1

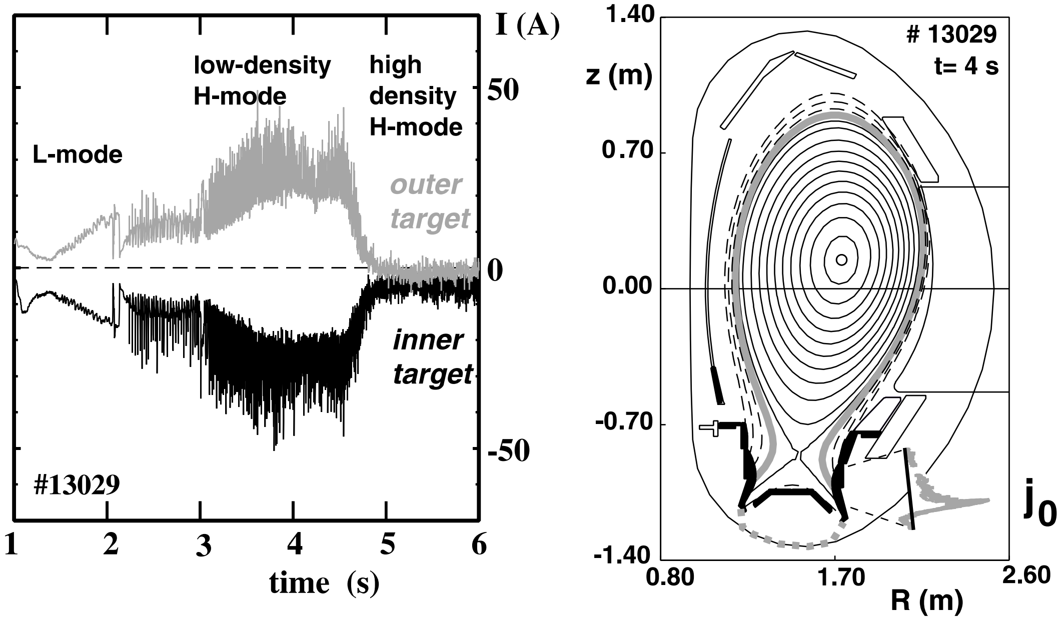

Fig. 1. Tile current measured in the inner and outer divertor and cross-section of ASDEX Upgrade. The field line plotted in grey is projected into the poloidal plane, it winds around the torus q times in toroidal direction and has a connection length of 40 m. Positive current flows out of the plate.

similar results. The shunt measurements, which integrate the current over a whole tile have low spatial resolution, but a very good signal to noise ratio. In addition, they are a cheap and very robust diagnostic.

3. Analytical model

The thermoelectric part of the measured current density j_0 is calculated using the analytical description developed by [2]. The SOL plasma is considered as an electric conductor, where a thermoelectric voltage caused by different contributions drives a parallel current, $j_\|$, which is limited by the resistivity of the field line. In the following, the label $\|$ is used for currents calculated with the analytical model. The thermoelectric current is carried by electrons flowing force-free along the field lines from the colder towards the hotter SOL ends, i.e., from the inner towards the outer divertor. For standard ASDEX Upgrade polarity (neg. toroidal field, lower single-null, ion ∇B-drift towards the divertor), this thermocurrent is in the direction of the plasma current. The thermocurrent-density is generally limited to the ion saturation current at the ion collecting (typ. the inner) plate, as long as no electrons are emitted out of the target. The contribution of PS currents to the total current at each target can be omitted because they cancel for each target individually, assuming vanishing plasma pressure at the upper and lower target ends. In the 1-D model, the SOL is unwound into a straight flux bundle of uniform width and oblique incidence. Connection length and angle of incidence are taken from the magnetic equilibrium reconstruction. A typical expansion factor between parallel flux densities in the midplane and perpendicular flux densities at the target surface is 30. With the field line pitch $B_\phi/B_p \approx 4$ in the outer midplane, we obtain target e-folding lengths being about 7.5 times longer than the corresponding midplane values. The connection length of a flux bundle between the inner and outer divertor is $L_{\rm con} = 60$ m close to the separatrix and $L_{\rm con} = 35$ m further outside.

The total SOL resistance is calculated using the resistivity $\eta_\| = 6.8 \times 10^{-4}\ T_e^{-3/2}\ Z_{\rm eff}^{0.78}$ (Ω m), where T_e is measured in eV. The $Z_{\rm eff}$ dependence is an approximation valid within the $Z_{\rm eff}$ range occurring in the SOL ($1 < Z_{\rm eff} < 4$). For constant pressure along the field line and $T_i = T_e$, the expected net current density between strike zones A and B with connected target plates and $T_{\rm A} < T_{\rm B}$ is [2,3]

$$j_\| = -\frac{1}{\overline{\eta}_\| L_{con}} T_{\rm A} \left\{ k' \left(\frac{T_{\rm B}}{T_{\rm A}} - 1 \right) + \ln \left[\frac{1 + j_\|/j_{s{\rm A}}}{(1 - \sqrt{T_{\rm B}/T_{\rm A}}\ j_\|/j_{s{\rm A}})^{T_{\rm B}/T_{\rm A}}} \right] \right\} \quad ({\rm A/m^2}), \quad (1)$$

where $j_{s{\rm A}}$ is the ion saturation current density. The term in wavy brackets assigns a voltage to a given temperature, therefore $T_{\rm A}$ has the dimension Volt, its numerical

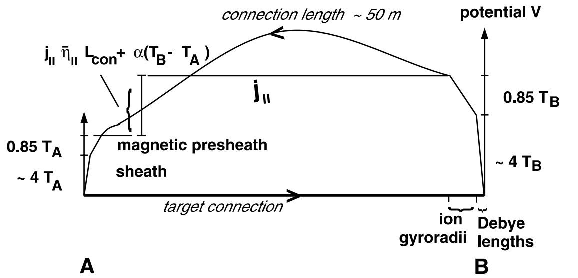

Fig. 2. Sketch of current flow and potential distribution for connected divertor target plates with low (A) and high (B) temperatures at the sheath.

value is calculated in eV. The situation is illustrated in Fig. 2. The coefficient $k' = (k + 0.85 - \alpha)$ contains different contributions to the net thermoelectric voltage: $k = 1/2\ln(4m_i/((1+Z)\pi m_e))$ is a measure for the ratio of the thermal speeds of electrons and ions, connected to the picture of fast electrons streaming to the wall ahead of the ions and causing a potential drop over the sheath. The value 0.85 is assigned to the potential drop in the presheath. α represents the thermo-voltage caused by the temperature gradient along the field line, and counteracts the effect of the sheath potentials. α contains ratios of Spitzer–Härm coefficients, $\alpha = 0.7$ for $Z = 1$, 0.91 for $Z = 2$ and 1.09 for $Z = 4$. In summary, we obtain the coefficients $k' = (3.68, 4.03, 3.96)$ for a pure (H, D, He) plasma. The logarithmic term in Eq. (1) represents the effect of the thermoelectric current on the sheath. For our conditions with $T_B > T_A$, $j_\parallel$ is negative, i.e., flowing from the plasma into the target A. j_{sA} is positive by definition [2], and therefore the ln term has a negative value. Its origin is the rise of the potential at the colder sheath and potential reduction at the hotter sheath due to the thermocurrent, reducing the potential difference and counteracting the effect of k'. For $T_B/T_A = 2$, it amounts to -1.76 for $j_\parallel/j_{sA} = -0.5$ and -3.1 for $j_\parallel/j_{sA} = -0.8$, which is no longer a small correction. Although Eq. (1) needs an iterative solution, one can clearly see that the normalized current $j_\parallel/j_{sA}$ cannot become more negative than -1. This is due to the fact that the thermocurrent is carried by – and therefore limited to – the ion flux at the low temperature side.

For the calculation of the SOL current radial distribution according to Eq. (1), a realistic T_e distribution is needed. This is obtained from a simple analytic solution of the parallel heat conduction equation

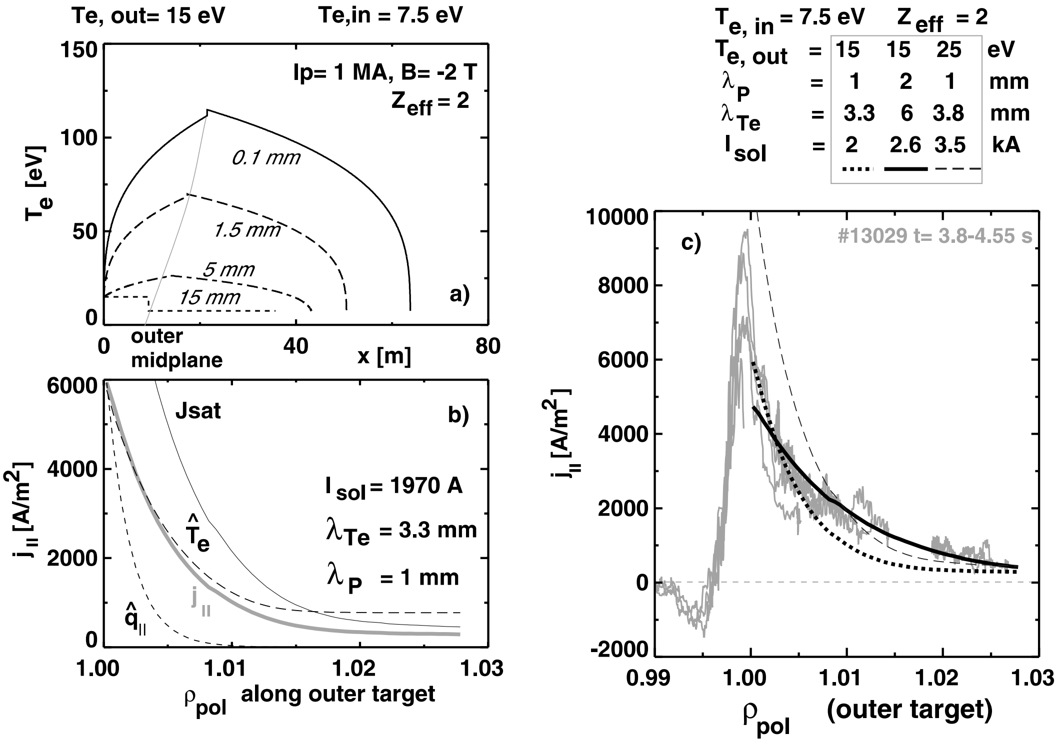

Fig. 3. Calculation of the SOL current distribution with the analytical model: (a) T_e distribution along the field lines from Eq. (3) for different distances from the separatrix; (b) thermocurrent from Eq. (1), ion saturation current and normalized T_e and parallel heat flux profiles; (c) comparison of thermocurrent profile for different model parameters with the measured profile in an H-mode discharge. The SOL region shown corresponds to about 1.5 cm in radial direction in the outer midplane and 15 cm along the target.

$$q_{\|} = -\kappa_0 T_e^{5/2} \frac{\partial T_e}{\partial x} \approx -2390 \frac{J}{sm\ \mathrm{eV}^{7/2}} Z_{\mathrm{eff}}^{-0.3} T_e^{5/2} \frac{\partial T_e}{\partial x}, \qquad (2)$$

$$T_e(x) = \left(T_{e,sh}^{7/2} + \frac{7}{2} \kappa_0^{-1} q_{\|} x \right)^{2/7}, \qquad (3)$$

where T_e is in eV. The Coulomb logarithm $\ln \lambda = 13$ was used to calculate κ_0, the Z_{eff} dependence is a fit for the Z-dependent numerical factor and the collision time contributing to κ_0. The calculation of the T_e distribution starts at the sheath, $x = 0$, with the parallel heat flux and T_e at the target as input. Z_{eff} is taken as constant, j_s is then calculated from $T_e(x)$ and the midplane electron density as additional input assuming constant pressure along the field line. An example for the analytical model and comparison with the experimental profile is shown in Fig. 3.

The agreement of the analytical model with the (ELM-averaged) measurements is good, except close to the separatrix, where the PS currents contribute to j_0, which are not taken into account in the model. The absolute value depends sensitively on the divertor temperature, while the shape is mainly determined by the midplane temperature decay length, which is between 3 and 6 mm following this analysis. The electron temperature is assumed to be constant along the inner and outer target plates in Fig. 3, which is not in contradiction to the Langmuir probe evaluation. The midplane T_e profile and the whole temperature distribution in the model results from the power flux in the inner and outer divertor sheaths ($P_{\mathrm{in}} = 0.9$ MW, $P_{\mathrm{out}} = 1.6$ MW). The total heating power of the discharge is $P_{\mathrm{heat}} = 5$ MW. Further inputs are the separatrix density $n_{e,\mathrm{sep}} = 3 \times 10^{19}\ \mathrm{m}^{-3}$ and the density e-folding length $\lambda_n = 0.023$ m taken from the experiment. The choice of the sheath power flux is somewhat arbitrary due to the neglect of radiation, but this has no big impact on the results due to the relatively weak ($P^{0.3}$) power dependence of $I_{\|}$ in the analytic model.

4. Scaling relations

The dependence of the thermocurrents on global plasma parameters was investigated by regression analysis of time slices of type-I ELMy H-mode discharges averaged over many ELMs. The currents used here refer to the total current measured in the inner divertor. The values have been extrapolated based on the measurements in one column of tiles in sector 14 under the assumption of toroidal symmetry. This assumption could be confirmed by comparison with two additional measurements available in sectors 4 and 12 equipped with lower amplification and S/N ratio. The most pronounced parametric dependence found is that on the Greenwald factor, $-I_0 \propto f_{\mathrm{Green}}^{-2.3}$, see Fig. 4. In a more refined regression analysis, we obtain

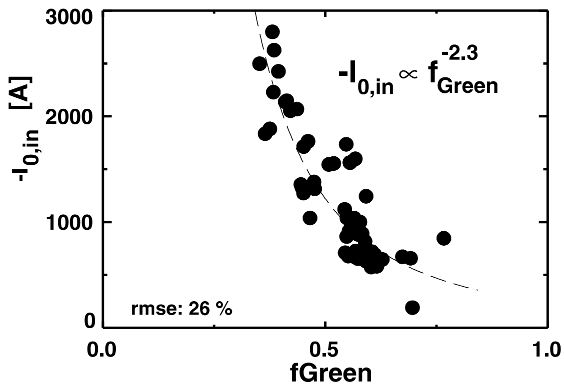

Fig. 4. Measured total electric current out of the inner target as a function of the Greenwald factor (left), $f_{\mathrm{Green}} = \overline{n}_e / n_e^{\mathrm{Green}}$ for various experimental conditions in type-I ELMy H-modes.

$$I_0^{\mathrm{sep-scale}} \propto n_{e,\mathrm{sep}}^{-2} I_p^{0.7} P_{\mathrm{heat}}^{0.35} q_{95}^{-0.9}. \qquad (4)$$

We use here the midplane separatrix density measured by the lithium beam diagnostic, since this is closer connected to divertor physics than $\overline{n}_e$. The separatrix density approaches $\overline{n}_e$ with increasing Greenwald factor according to $n_{e,\mathrm{sep}}/\overline{n}_e \propto f_{\mathrm{Green}}^{0.24}$. With rising density, the thermocurrent profile broadens and shifts outward. No significant dependence on $\overline{Z}_{\mathrm{eff}}$ could be derived from the experimental data, which may be due to the fact that Z_{eff} in the SOL behaves quite differently from $\overline{Z}_{\mathrm{eff}}$. Also, the influence of main chamber recycling derived from the H_α flux [8] on the thermocurrent is found to be weak, suggesting that the corresponding part of the SOL electron density profile is too far outside the separatrix.

5. Discussion

The good agreement of the analytical model with the thermoelectric part of the SOL currents allows to derive SOL temperatures with moderate accuracy, but relatively low experimental effort. Since the current profile at the target plate turns out to be sensitive against the midplane decay length under the assumption of classical parallel conductivity, the flux expansion along the target plate allows to resolve midplane e-folding lengths in the mm range. The strong reduction of the currents while approaching the Greenwald density reflects the cooling of the divertor plasma. To compare the experimental scaling for the target-integrated currents with that obtained from the analytical model, we need an ansatz for the variation of the divertor temperatures with density. For the configuration used, the inner divertor is the colder one, i.e., label A in Eq. (1) corresponds to the inner and label B to the outer divertor in the following. We chose $T_{e,\mathrm{out}} \propto (n_{e,\mathrm{sep}}/n_{e,\mathrm{Green}})^{-2}$, $T_{e,\mathrm{in}} = T_{e,\mathrm{out}}/2$. With this ansatz, the current is calculated with the analytical model for various parameter sets in the vicinity of the experimental conditions of Fig. 3, resulting in the analytical scaling

$$I_{\parallel}^{\mathrm{analyt-scale}} \propto n_{e,\mathrm{sep}}^{-1.3} I_p^{0.5} P_{\mathrm{heat}}^{0.3} q_{95}^{-0.95} Z_{\mathrm{eff}}^{-0.3}. \quad (5)$$

This is quite similar to the experimental scaling, suggesting that the ansatz for $T_{e,\mathrm{div}}$ is reasonable. The q_{95} dependence is nicely reconciled and therefore attributed to the change of field line length. The inferred positive influence of I_p on the divertor temperature (via $n_{e,\mathrm{Green}}$) suggests the importance of this parameter on SOL transport in the H-mode. The dependence on Z_{eff} is not found in the experimental data, but one has to keep in mind that here only a line-averaged value (dominated by the central plasma) was available, and the corresponding Z_{eff} in the SOL may behave differently, in particular during density variations.

An open question remains whether the SOL currents have an impact on edge stability or H-mode performance. Taking a current of 3 kA flowing force-free along the field lines from the outer into the inner divertor, the current winds q times around the torus leading to, e.g., 12 kA net current in the direction of the plasma current. These currents, which are not considered self-consistently in the magnetic reconstruction so far, have an impact on the magnetic shear, in particular, in the X-point region where the equilibrium poloidal field is small. Work is in progress to assess the impact of the additional currents on edge ballooning stability and the H-mode threshold.

References

[1] P. Harbour, D. Summers, S. Clement et al., J. Nucl. Mater. 162–164 (1989) 236.
[2] G.M. Staebler, F.L. Hinton, Nucl. Fus. 29 (1989) 1820.
[3] A.V. Chankin, S. Clement, L. de Kock, S.K. Erents, P.J. Harbour, J. Nucl. Mater. 196–198 (1992) 739.
[4] M. Schaffer, A. Chankin, H. Guo, G. Matthews, R. Monk, Nucl. Fus. 37 (1997) 83.
[5] N. Asakura, S. Sakurai, N. Hosogane, M. Shimada, K. Itami et al., Nucl. Fus. 39 (1999) 1983.
[6] C.S. Pitcher, P.C. Stangeby, Plasma Phys. Controlled Fusion 39 (1997) 779.
[7] A.V. Chankin, J. Nucl. Mater. 241–243 (1997) 199.
[8] A. Kallenbach, D. Coster, J.C. Fuchs, H.Y. Guo, G. Haas et al., Plasma Phys. Controlled Fusion 41 (1999) B177.